

## <sup>18</sup>F-FDG PET/CT in diagnosis of skeletal metastases

LI Na<sup>1</sup> LI Yaming<sup>1,\*</sup> YANG Chunming<sup>2</sup> LI Xuena<sup>1</sup> YIN Yafu<sup>1</sup> ZHOU Jiumao<sup>1</sup>

<sup>1</sup> Department of Nuclear Medicine, No.1 Hospital Affiliated to China Medical University, Shenyang 110001, China

<sup>2</sup> Department of Urinary, No.1 Hospital Affiliated to China Medical University, Shenyang 110001, China

**Abstract** This work is to evaluate correlated lesions in PET and CT images of patients suffering skeletal metastases so as to improve efficacy of <sup>18</sup>F-FDG PET/CT in diagnosing bone metastases. PET and CT images of 25 patients with malignant tumor suspected bone metastases were reviewed independently by three experts. A region of interest was placed over each lesion, and the standardized uptake value (SUV) was calculated at the maximal single pixel value. The *t* and  $\chi^2$  tests were used for statistical analysis. Of the 203 lesions detected on the PET and CT images, 189 were malignant and 14 were benign lesions. PET alone identified 159 malignant lesions and 6 benign lesions, CT alone identified 152 malignant lesions and 11 benign lesions. For PET, the diagnostic sensitivity, specificity and accuracy were 84.1%, 71.4% and 83.3%, respectively, while 80.4%, 71.4% and 83.3% for CT. No significant difference was found between PET and CT in detecting bone metastases ( $\chi^2=0.89, 0.19, 0.59, P>0.05$ ). Statistical difference of positive ratio of PET was found between osteoblastic and osteolytic or mixed lesions ( $\chi^2=47.33, 7.93, \text{both } P<0.05$ ). Of the 122 positive lesions on both CT and PET scan, the mean SUV was  $5.76\pm 3.41, 8.52\pm 5.37$  and  $7.78\pm 4.96$  in osteoblastic lesions, osteolytic lesions and mixed lesions, respectively. Significant difference was found between osteoblast lesions and osteolytic lesions ( $t=2.28, P<0.05$ ). PET images alone may leave out half of osteoblastic lesions, but combined analysis of PET and CT images gives better diagnosis.

**Key words** <sup>18</sup>F-FDG, PET/CT, Neoplasm, Bone metastases

### 1 Introduction

The skeletal system is commonly seen (just after the lung and liver) as distant metastasis of malignant tumors, among which solid tumors exhibit higher rate of metastasis in the skeletal system<sup>[1]</sup>. Bone metastases occur in up to 70% of patients with advanced breast cancer, and 15%–30% patients with carcinomas of the lung, colon, stomach, bladder, uterus, rectum, thyroid or kidney<sup>[2]</sup>. Early detection or exclusion of bone metastases is of high clinical importance in management of the patients. Bone metastases was detected with <sup>99m</sup>Tc methylenediphosphonate scintigraphy, a common means of detecting bone metastases, with variable diagnostic sensitivity and low specificity<sup>[3]</sup>. Nowadays, <sup>18</sup>F-fluorodeoxyglucose (FDG) positron emission tomography (PET) becomes

popular. Whole-body PET imaging is able to detect metastases at different sites and organs in a single examination. It has been recognized that <sup>18</sup>F-FDG PET is more sensitive than conventional bone scan in detecting bone metastases<sup>[4]</sup>. And combined PET/CT scanners have been in rapid clinical applications. This work was to prospectively compare the <sup>18</sup>F-FDG uptake feature and corresponding CT morphology of each bone metastases lesion in a hybrid PET/CT, as well to improve the diagnostic accuracy of the PET/CT.

### 2 Materials and methods

#### 2.1 Patients

Twenty-five patients (14 males, 11 females, age: 35–72), with pathology-proven malignancies of lung

\* Corresponding author. E-mail address: ymi2001@163.com

Received date: 2009-05-08

(15), breast (4), prostate (2), rectal (1), lymphoma (1), ovarian (1), and nasopharyngeal (1) carcinomas bone metastases, underwent  $^{18}\text{F}$ -FDG PET/CT.

## 2.2 $^{18}\text{F}$ -FDG PET/CT imaging

The patients fasted for at least 4 h before the  $^{18}\text{F}$ -FDG PET/CT study. Fifty minutes before scanning, they received a blood glucose level checked ( $<10$  mmol/L) and an intravenous injection of  $^{18}\text{F}$ -FDG (5.55 MBq/kg). After injection, they were asked to remain at rest before their scan. All patients were asked to urinate just prior to scan. Half-body (from brain to mid thigh) PET and noncontrast-enhanced CT images were acquired using a hybrid PET/CT system (Discovery LS; GE Healthcare Technologies). Transaxial PET images were acquired with an intersection spacing of 4.25 mm. CT images were acquired with a 4.25-mm section thickness, at 140 kV 80 mA. PET, CT, and fused PET/CT images were available for review.

## 2.3 Image analysis

PET/CT images were reviewed independently by two experienced nuclear medicine physicians, and one radiologists who had no knowledge of any clinical information. The temporal changes in  $^{18}\text{F}$ -FDG uptake of these metastases lesions were investigated semiquantitatively as measured by maximum standardized uptake value ( $\text{SUV}_{\text{max}}$ ) by a region of interest at each lesion, and the maximal SUV was calculated at the maximal single pixel value<sup>[5]</sup>. On the PET images, the presence of bone metastasis was diagnosed on the basis of localized moderate or marked bony  $^{18}\text{F}$ -FDG uptake, combining the distribution and type of concentrations. For spinal column, lesions located at the pedicle of vertebral arch and/or vertebral body were considered as malignant, whereas localized along the plane of the disk space, or at a facet joint with mild abnormal increased activity were considered benign<sup>[6]</sup>. Lytic, sclerotic, mixed lytic- sclerotic, intramedullary changes (loss of bone marrow fat) or bone lesions with accompanying adjacent soft tissue abnormality on the CT images were considered malignancy<sup>[7]</sup>.

The final diagnosis was based on other following up imaging studies in 6 month. Of all the 25 patients, 2 underwent follow-up PET/CT scan, 3 underwent

radiography and bone scan, 12 underwent separate diagnostic CT, 3 underwent MR imaging, 5 underwent bone scan. Malignant were verified with progressive findings in the following images.

## 2.4 Statistical analysis

Location-based sensitivity of PET and CT was assessed by using the  $\chi^2$  test. The *t* test was used to assess the differences in  $^{18}\text{F}$ -FDG uptake intensity ( $\text{SUV}_{\text{max}}$ ) in different group of bone lesions.  $P < 0.05$  were considered to indicate statistical significance.

## 3 Results

On the  $^{18}\text{F}$ -FDG PET/CT images of the 25 patients, 203 bone lesions were found, of which 189 were diagnosed as metastases (Table 1), and 14 were benign lesions, including 7 degeneration, 3 compressive fracture, 2 bone cyst and 2 bone tuberculosis. By PET alone, 159 malignant and 6 benign lesions were accurately diagnosed, but it lost 30 malignant lesions (29 osteoblastic, and 1 osteolytic) and mistook 4 benign lesions as malignant (Figs.1–5). The sensitivity of single PET was 84.1% (159/189), the specificity was 71.4% (10/14) and the accuracy was 83.3% (169/203). CT scan defined 152 malignant lesions classified as osteolytic (85), osteoblastic (58) and mixed-pattern (9) and 11 benign lesions, except that 37 malignant lesions were absent and 3 benign lesions were taken for malignant. The sensitivity, specificity and accuracy of CT alone was 80.4% (152/189), 78.6% (11/14) and 80.3% (163/203), respectively. No significant difference was found between the bone metastasis diagnosis by PET and CT ( $\chi^2 = 0.89, 0.19, 0.59, P > 0.05$ ).

In the 189 diagnosed metastatic lesions, 122 demonstrated concordant positive PET and CT findings classified as osteoblastic (29), osteolytic (84) and mixed-pattern (9). The majority of osteolytic (84/85, 98.8%) and all mixed-pattern (9/9, 100%) lesions, and some osteoblastic lesions (29/58, 50%), showed increased  $^{18}\text{F}$ -FDG uptake. PET detected fewer lesions in the subgroup with osteoblastic disease compared with those with purely osteolytic or mixed-pattern disease ( $\chi^2 = 47.33, P < 0.01; \chi^2 = 7.93, P < 0.01$ ).

**Table 1** Bone metastases found in PET and CT images of 25 patients.

PET images	CT images				Total
	Osteoblastic	Osteolytic	Mixed	Negative	
Positive	29	84	9	37	159
Negative	29	1	0	0	30*
Total	58	85	9	37	189

Note: CT positive but PET negative

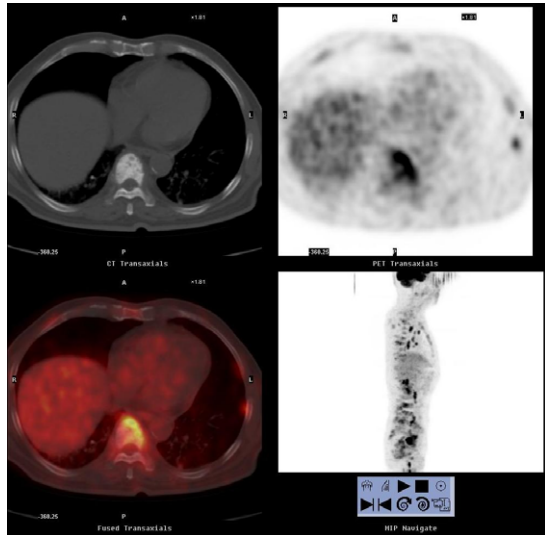


**Fig.1** Metastatic Pattern A. Images in 72-year-old man with prostate cancer. Focal intense FDG uptake is seen in thoracic spine, where osteoblastic changes are depicted at CT.

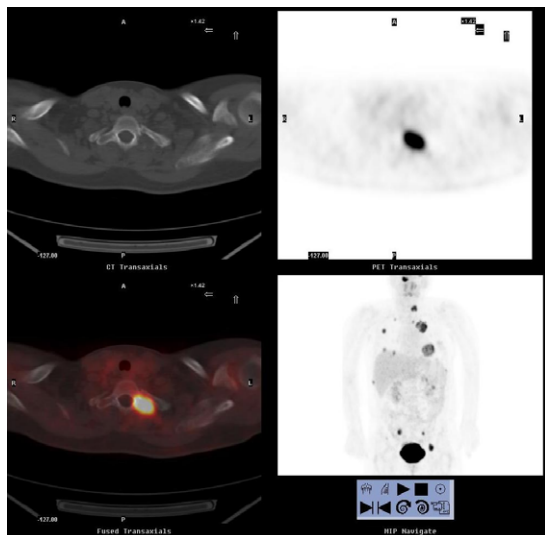


**Fig.2** Metastatic Pattern B. Images in 35-year-old woman with breast cancer. There is an FDG-avid soft-tissue mass in the transversal process of thoracic vertebra, and soft-tissue mass formation and bone destruction are both seen at CT.

For the 29 <sup>18</sup>F-FDG-avid osteoblastic lesions, the mean SUV<sub>max</sub> (±standard deviation) was 5.76±3.41.

For the 84 <sup>18</sup>F-FDG-avid osteolytic lesions and 9 <sup>18</sup>F-FDG-avid mixed-pattern lesions, the mean SUV<sub>max</sub> was 8.52±5.37 and 7.78±4.96, respectively. The osteolytic lesions had higher SUV<sub>max</sub> compared with osteoblastic lesions ( $t=2.28, P<0.05$ ). The differences between osteoblastic and mixed-pattern lesions, osteolytic and mixed lesions were not significant ( $t=0.84, 0.17, P>0.05$ ). For the 37 lesions diagnosed as bone metastases without CT morphologic changes also had high <sup>18</sup>F-FDG uptake, with a mean SUV<sub>max</sub> of 7.36±4.13.

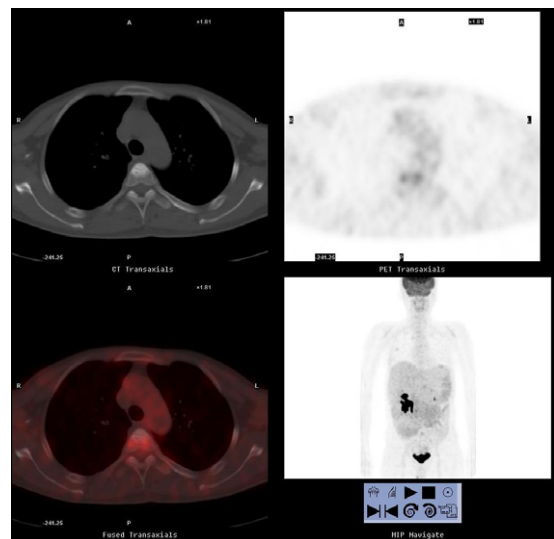


**Fig.3** Metastatic Pattern C. Images in 43-year-old man with lung cancer. Osteoblastic changes are depicted at CT, but focal intense FDG uptake is not seen in the thoracic spine metastases.

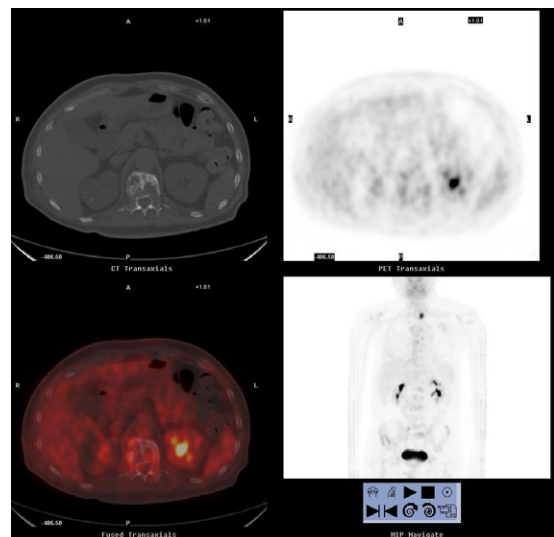


**Fig.4** Metastatic Pattern D. Images in 65-year-old man with rectal cancer. Osteolytic change is one of the typical features of bone metastasis from renal cancer, but non-FDG-avid tumor can be seen at the same place.

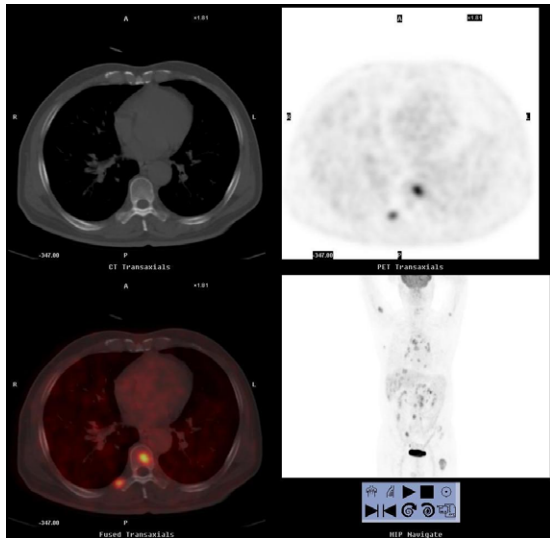


**Fig.5** Metastatic Pattern E. Images in 68-year-old man with history of lymphoma. PET showed focal intense metabolic activity in the thoracic vertebra., but nodefinite morphologic abnormalities are observed on the CT image.

#### 4 Discussion

Early detection of bone metastases allows for early therapy and subsequent reduction in the morbidity rate. The diagnostic gold standard of most malignant tumors was pathology, but it is ethically unacceptable to obtain multiple bone biopsies for tissue verification. Pomeranz S J, *et al*<sup>[8]</sup> postulated that typical imaging appearance, combining various imaging results with clinical following-up in untypical lesions could be the gold standard for diagnosing bone metastases. According to the criteria, 189 lesions of 203 lesions in the 25 patients were diagnosed as malignant, and 14 were benign.

It was previously reported that  $^{18}\text{F}$ -FDG PET is superior to conventional imaging procedures for detecting distant metastases, but PET and CT provided similar diagnostic accuracy<sup>[9]</sup>. Our results indicated that PET is the superior modality than CT, but no significant difference was found between PET and CT in diagnosing bone metastases.

In PET the images, the glucose transport level in the cellular membrane and cellular glycolysis affected concentration and retention of the  $^{18}\text{F}$ -FDG. Many benign lesions, such as reactive tuberculosis, compressive fracture, and recovery stage after trauma may show similar  $^{18}\text{F}$ -FDG uptakes to malignant lesions. In our study, with PET alone, 4 lesions were mistaken as bone metastases. Two of them were

compressive fracture, while the other 2 lesions were pleural involvement rather than bone metastases. On the other hand, most of the lesions mistaken by the PET scan were osteoblastic, which would evoke an effect on osteocyte but no occupying marrow for bone repair were predominant<sup>[10]</sup>. Therefore, PET alone was incorrect in determining this kind of lesions, but specificity of the PET interpretation could be improved by the CT images in PET/CT, which showed degenerative changes in locations corresponding to areas of increased  $^{18}\text{F}$ -FDG uptake, and revealed that areas with increased uptake and suspected of being skeletal were actually uptake by soft tissues. In addition, the primary tumor cells may seem different during metastases and show a pathological utilization of glucose, and thus lose the storage of glucose in the metastases. So the sensitivity of  $^{18}\text{F}$ -FDG PET for metastases to bone appears to be lower than to other organs.

Tiny tumors hidden in the marrow was undetectable at early stage with CT scan owing to uncharacteristic morphologic conversion. However, as enhanced glycolysis prior to osteocyte reaction frequently appeared in this kind of foci, glucose uptake by the tumor can be measured by  $^{18}\text{F}$ -FDG PET, hence the greater possibility of detecting early stage metastases that are confined to bone marrow, and may precede the cortical bony changes to be detected by CT<sup>[11]</sup>. Our data show that combining PET images, mostly malignant lesions seen as normal with CT were diagnosed accurately. Besides, CT detects mainly cortical destructions, which are difficult to differentiate with osteoporosis and degenerative changes. In current study, three degenerative lesions were mistaken as malignant lesions with CT imaging alone. The metabolic activity of the lesions in PET scan must be valuable in the diagnosis of the equivocal lesions in CT.

In the 189 malignant lesions, PET detected most lesions that were osteolytic and in mixed-pattern on CT, while osteoblastic metastases with lower metabolic activity were frequently undetectable by PET. For lesions of increased uptake with abnormal CT, osteolytic metastases have greater avidity for  $^{18}\text{F}$ -FDG than osteoblastic lesions. PET has great sensitivity to osteolytic and mixed-pattern lesions,

which contain more tumor cellularity, and have higher glycolytic rate that may have an influence on  $^{18}\text{F}$ -FDG concentrations. In addition, more aggressive, osteolytic lesions might be expected to outstrip its blood supply, which renders the tumor more hypoxic than osteoblastic lesions. Hypoxia increases  $^{18}\text{F}$ -FDG uptakes in some cell lines, and this may be an additional factor in osseous metastasis accumulation<sup>[12]</sup>.

Cook G J, *et al.*<sup>[10]</sup> evaluated metabolic activity in osteoblastic and osteolytic lesions by  $^{18}\text{F}$ -FDG, and found that avidity of  $^{18}\text{F}$ -FDG was related to morphologic appearance of bone metastases, but not intrinsic to the tumor type. They also found that the survival rate from the time of diagnosis of bone metastases in those with purely osteolytic disease was lower than a group with either sclerotic or mixed-pattern lesions. Du and coworkers<sup>[13]</sup> performed  $^{18}\text{F}$ -FDG PET/CT before and after therapy in 25 tumor patients with bone metastases. The temporal changes in  $^{18}\text{F}$ -FDG uptake and corresponding CT morphology features identified in the 25 patients were followed up and correlated with therapeutic outcome retrospectively. After treatment, 76.4% of  $^{18}\text{F}$ -FDG avid lesions became  $^{18}\text{F}$ -FDG negative. However, most of them remained abnormal on CT, with predominantly osteoblastic appearance. Some lesions appeared osteolytic or CT-negative before therapy gradually became osteoblastic with sequential imaging.  $^{18}\text{F}$ -FDG uptakes reflect the immediate tumor activity of bone metastases, and serial  $^{18}\text{F}$ -FDG PET/CT is useful in monitoring bone metastases response to anticancer therapy.

## 5 Conclusion

We should aware that PET images are usually difficult to identify small or hypometabolic lesions and localize them accurately to the skeleton because of the limited

spatial resolution of the technique. On the other hand, small morphologic changes at CT are common, but it is difficult to make a definite diagnosis of bone metastases. In hybrid PET/CT images, the information of PET and CT was complementary, morphologic changes and corresponding precise localization combination with elevated  $^{18}\text{F}$ -FDG uptakes must be able to improve the sensitivity and specificity, thus make the diagnosis of bone metastases accurately.

## References

- 1 Ghanem N, Uhl M, Brink I, *et al.* *Eur J Radiol*, 2005, **55**: 41–55.
- 2 Chen Y W, Huang M Y, Hsieh J S, *et al.* *Kaohsiung J Med Sci*, 2007, **23**: 639–646.
- 3 Fogelman I, Cook G, Israel O, *et al.* *Semin Nucl Med*, 2005, **35**: 135–142.
- 4 Bohdiewicz P J, Wong C Y O, Kandas D, *et al.* *Clin Nucl Med*, 2003, **28**: 966–970.
- 5 Nakamoto Y, Cohade C, Tatsumi M, *et al.* *Radiology*, 2005, **237**: 627–634.
- 6 Evan-Sapir E, Master U, Flusser G, *et al.* *J Nucl Med*, 2004, **45**: 272–278.
- 7 Metser U, Lerman H, Blank A, *et al.* *J Nucl Med*, 2004, **45**: 279–284.
- 8 Pomeranz S J, Pretorius H T, Ramsingh P S. *Semin Nucl Med*, 1994, **24**: 188–207.
- 9 Mahner S, Schirmacher S, Brenner W, *et al.* *Ann Oncol*, 2008, **19**: 1249–1254.
- 10 Cook GJ, Houston S, Rubens R, *et al.* *J Clin Oncol*, 1998, **16**: 3375–3379.
- 11 Even-Sapir E, Metser U, Mishani E, *et al.* *J Nucl Med*, 2006, **47**: 287–297.
- 12 Clavo AC, Brown RS, Wahl R L. *J Nucl Med*, 1995, **36**: 1625–1632.
- 13 Du Y, Cullum I, Illidge T M, *et al.* *J Clin Oncol*, 2007, **25**: 3440–3447.